

## REPORT No. 365

### AERODYNAMIC CHARACTERISTICS OF CIRCULAR-ARC AIRFOILS AT HIGH SPEEDS

By L. J. BRIGGS and H. L. DRYDEN

#### SUMMARY

The aerodynamic characteristics of eight circular-arc airfoils at speeds of 0.5, 0.65, 0.8, 0.95, and 1.08 times the speed of sound have been determined in an open-jet air stream 2 inches in diameter, using models of 1-inch chord. The lower surface of each airfoil was plane; the upper surface was cylindrical. As compared with the measurements described in N. A. C. A. Technical Report No. 319 (Reference 1), the circular-arc airfoils at speeds of 0.95 and 1.08 times the speed of sound are more efficient than airfoils of the R. A. F. or Clark Y families. At a speed of 0.5 times the speed of sound, the thick circular-arc sections are extremely inefficient, but thin sections compare favorably with those of the R. A. F. family. A moderate rounding of the sharp edges changes the characteristics very little and is in many instances beneficial. The results indicate that the section of the blades of propellers intended for use at high tip-speeds should be of the circular-arc form for the outer part of the blade and should be changed gradually to the R. A. F. or Clark Y form as the hub is approached.

#### INTRODUCTION

In the course of the measurements of the aerodynamic characteristics of the 24 airfoil sections described in Technical Report No. 319 (Reference 1) of the National Advisory Committee for Aeronautics, the authors found that it was advantageous to move the maximum ordinate of the section further back from the leading edge as the speed was increased. A segment of a circular cylinder with the maximum ordinate at 50 per cent of the chord was found to be more efficient at high speeds than airfoil sections of the R. A. F. or Clark Y families of the same thickness. It was deemed desirable to determine whether this increased efficiency at high speed is characteristic of circular-arc sections of all the thickness ratios from 0.08 to 0.20 times the chord and to determine the effect of rounding the sharp edges, which would be necessary in practice. These were the objects of the work now to be described. The measurements were carried out at the National Bureau of Standards with the cooperation and financial assistance of the National Advisory Committee for Aeronautics.

#### APPARATUS AND EXPERIMENTAL PROCEDURE

Airfoils.—The sections of the 8 airfoils used are shown in Figure 1. Each airfoil had a chord length of 1 inch and was 6 inches long. In conformity with the notation adopted in Technical Report 319 (Refer-

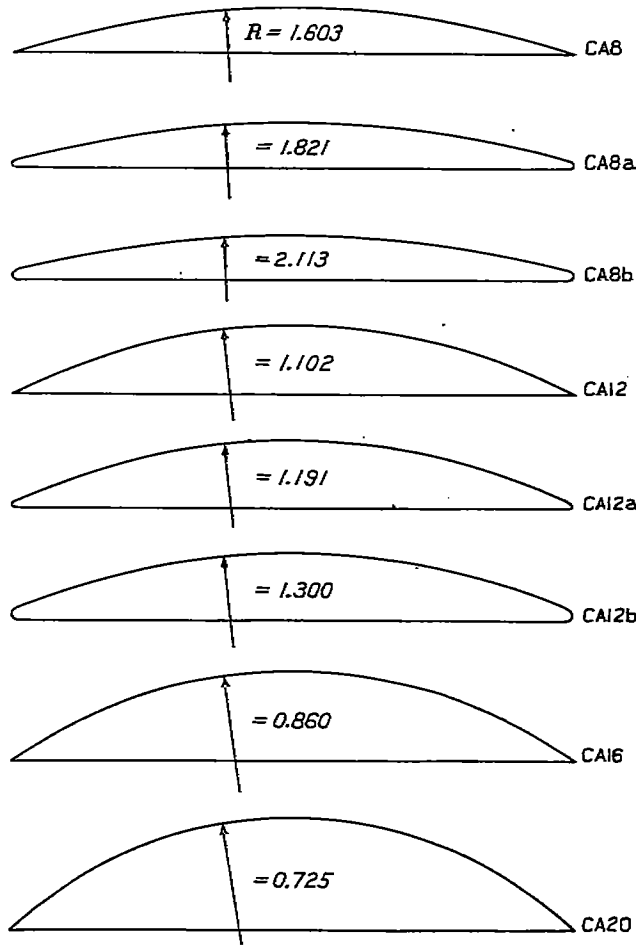


FIGURE 1.—The airfoil sections

ence 1), the circular-arc sections are indicated by the capital letters CA. The number following denotes the thickness in hundredths of the chord length, and the small letters following the number refer to the degree of rounding of the edges. When the leading and trailing edges of the section are sharp, no small letter is used. The letter a denotes the height of

the circular-arc above the lower surface at the leading and at the trailing edge is 0.01 times the chord length; the letter b denotes that the height is 0.02 times the chord length. CA8 is the airfoil called "circular-arc airfoil" in Technical Report No. 319.

**Air stream, balance, nozzles.**—The equipment used is described in detail in Technical Report No. 319. The airfoils were mounted so as to span the cylindrical air stream, which was 2 inches in diameter. Measurements were made at speeds of  $0.5c$ ,  $0.65c$ ,  $0.8c$ ,  $0.95c$ , and  $1.08c$ , where  $c$  denotes the speed of sound at the temperature of the jet. At  $20^\circ\text{C}$ ,  $c$  is 1,126 feet per second, and the corresponding airspeeds were 563, 732, 902, 1,071, and 1,218 feet per second.

#### Reduction of observations.—

##### NOTATION

- $p_t$  = absolute static pressure inside approach pipe (velocity pressure negligible)
- $p_o$  = absolute static pressure in jet (equal to barometric pressure)
- $p_t - p_o$  = impact pressure
- $V$  = speed of air in jet
- $c$  = speed of sound at temperature of jet
- $c_0$  = speed of sound at  $0^\circ\text{C}$
- $\rho$  = density of air in jet
- $\frac{1}{2}\rho V^2$  = velocity pressure
- $J$  = mechanical equivalent of heat
- $C_p$  = specific heat of air at constant pressure
- $k$  = ratio of specific heats
- $C_L$  = lift coefficient
- $C_D$  = drag coefficient
- $A$  = area of airfoil taken as chord times exit diameter of nozzle.
- $L$  = lift
- $D$  = drag

The following relations are derived in N. A. C. A. Technical Report No. 255 (Reference 2):

$$\frac{V^2}{c^2} = \frac{546 J C_p}{c_0^2} \left\{ \left( \frac{p_t}{p_o} \right)^{\frac{k-1}{k}} - 1 \right\}$$

$$\frac{1}{2}\rho V^2 = \frac{288 \times 0.0012255}{1013300} J C_p p_o \left\{ \left( \frac{p_t}{p_o} \right)^{\frac{k-1}{k}} - 1 \right\}$$

$$\frac{p_t - p_o}{\frac{1}{2}\rho V^2} = \frac{(1 + 0.19991 V^2/c^2)^{1/2} - 1}{3.5088 \times 0.19991 V^2/c^2}$$

The lift and drag coefficients are defined by the equations:

$$C_L = \frac{L}{\frac{1}{2}\rho V^2 A}$$

$$C_D = \frac{D}{\frac{1}{2}\rho V^2 A}$$

The quantities  $V/c$ ,  $C_L$ , and  $C_D$  were computed by means of these equations from the observed lift and drag, the pressure inside the approach pipe, and the barometric pressure.

#### RESULTS AND DISCUSSION

The results are given in the form of polar diagrams in Figures 2 to 9, inclusive. Numerical values of the lift and drag coefficients for various angles of attack are given in Table I.

A comparison of Figures 2, 3, and 4 and of Figures 5, 6, and 7 shows that the effect of rounding the leading and trailing edges is small. The degree of rounding indicated by a produces very little effect, the differences at positive lifts being within the experimental error, except perhaps for a slight increase in the drag coefficient at high lift coefficients. The greater rounding of the b sections gives a further small increase in drag coefficient at high lift coefficients, but a perceptible decrease in the minimum drag coefficient. As a whole the rounding of the edges does not greatly modify the efficiency.

As with other sections, the effect of thickness is very great. The thicker sections are much less efficient at all speeds and the increase in drag coefficient with increasing speed is greater for the thick sections than for the thin.

Figures 10 to 29, inclusive, show the characteristics of circular-arc sections in comparison with airfoils of the R. A. F. and Clark Y families, the data for the latter being taken from N. A. C. A. Technical Report No. 319. Each figure contains the curves for a single speed and a single thickness ratio. Figure 10, for example, gives the curves for a thickness of 0.08 times the chord at a speed of 0.5 times the speed of sound. The circular-arc section is seen to compare favorably with the corresponding R. A. F. section except at high lift coefficients. It is not quite as efficient as the corresponding Clark Y section. Figures 11, 12, 13, and 14 give the curves for the same sections at speeds of  $0.65c$ ,  $0.8c$ ,  $0.95c$ , and  $1.08c$ . At a speed of  $0.8c$  (Figure 12), the circular-arc section is appreciably better over a large part of the working range than either of the other two. At a speed of  $0.95c$  (Figure 13), it is decidedly better, and at a speed of  $1.08c$  (Figure 14), the drag of the circular-arc section over a large part of the working range does not exceed 70 per cent of the drag of the Clark Y.

Comparisons for other thickness ratios may be made in like manner. Passing to Figures 25, 26, 27, 28, and 29 for a thickness of 0.20 times the chord, we find at low speeds (Figures 25 and 26) that the circular-arc section is extremely inefficient as compared with the corresponding R. A. F. and Clark Y sections. At a speed of  $0.65c$  (Figure 26), the circular-arc section begins to show an advantage at large lift coefficients. This is more pronounced at  $0.8c$  (Figure 27), and at speeds of  $0.95c$  and  $1.08c$  (Figures 28 and 29) the cir-

cular-arc section is the best over most of the working range. At a speed of  $1.08c$ , the drag of the circular-arc section within the working range does not exceed 80 per cent of the drag of the Clark Y section.

These results indicate that it would be beneficial to use circular-arc sections for the outer part of a propeller blade intended for use at high tip speeds, retaining sections of the conventional type nearer the hub where the thickness ratio is large and the speed low. The length over which the circular-arc section should be used depends upon the thickness of the blade and its intended tip speed. The results of these tests should in any case be supplemented by measurements on actual propellers at high tip speeds, and in such tests the best length could be determined. It seems not unreasonable to expect that a circular-arc section can be used profitably over the outer third of the blade.

#### CONCLUSIONS

It has been found that circular-arc sections are more efficient at high speeds than either R A. F. or Clark Y sections. A moderate rounding of the leading and trailing edges is not detrimental. It appears desirable to use circular-arc sections for the outer sections of propeller blades designed for use at high tip speeds.

#### ACKNOWLEDGEMENT

We wish to acknowledge the efficient assistance of Mr. P. S. Ballif in the conduct of the tests and in the computation of the results.

BUREAU OF STANDARDS,  
WASHINGTON, July, 1930.

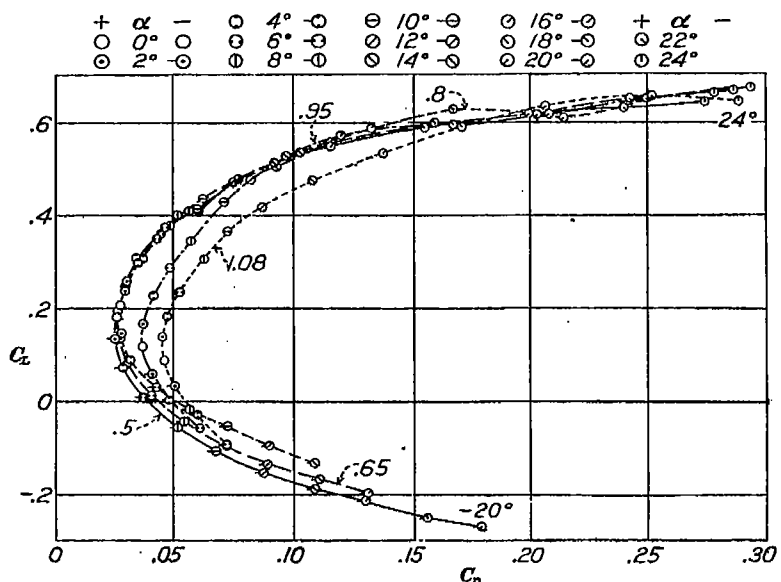


FIGURE 2.—Polar diagrams for airfoil CA8 for five values of  $V/c$

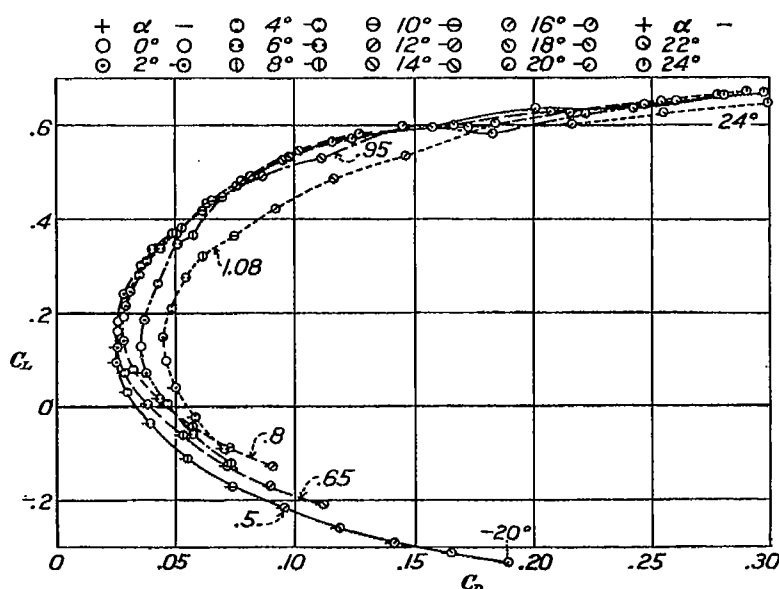


FIGURE 3.—Polar diagrams for airfoil CA8a for five values of  $V/c$

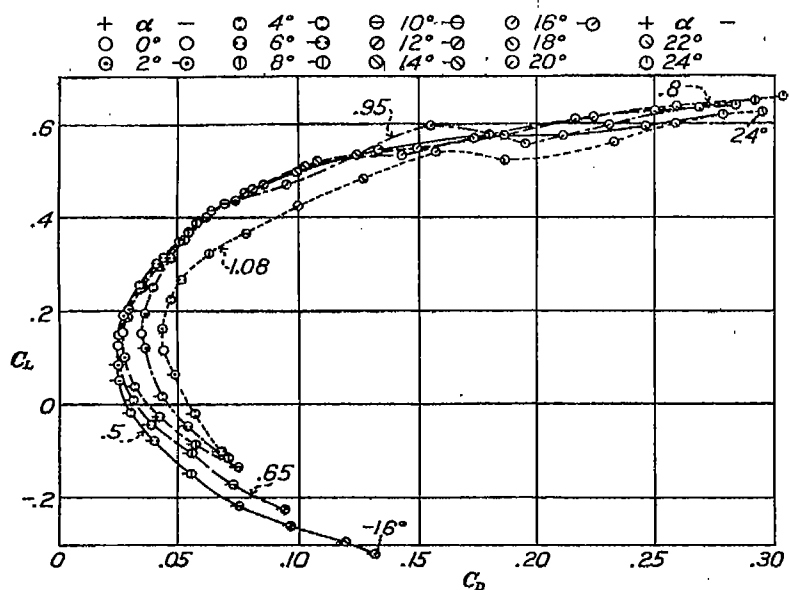


FIGURE 4.—Polar diagrams for airfoil CA8b for five values of  $V/c$

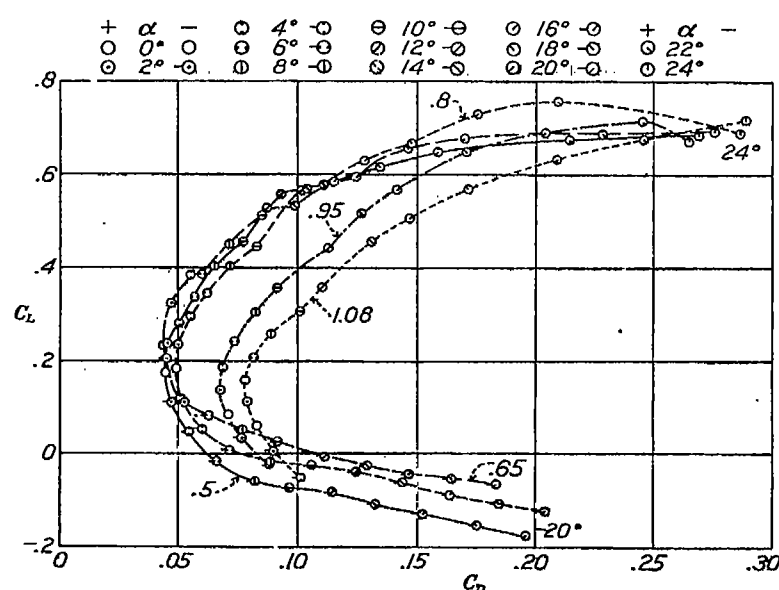


FIGURE 5.—Polar diagrams for airfoil CA12 for five values of  $V/c$

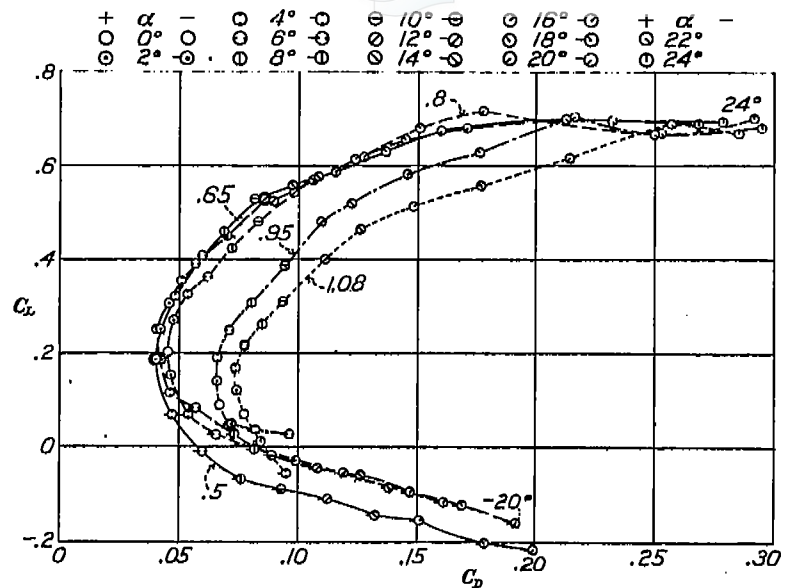


FIGURE 6.—Polar diagrams for airfoil CA12a for five values of  $V/c$

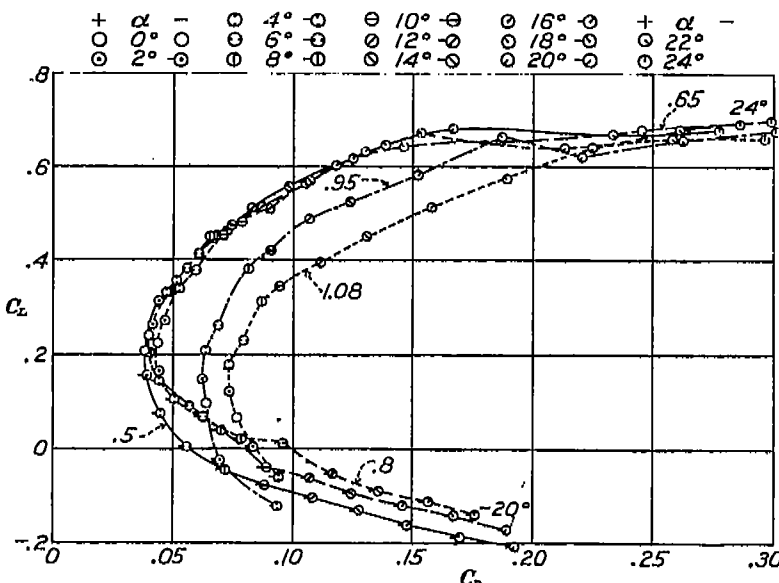


FIGURE 7.—Polar diagrams for airfoil CA12b for five values of  $V/c$

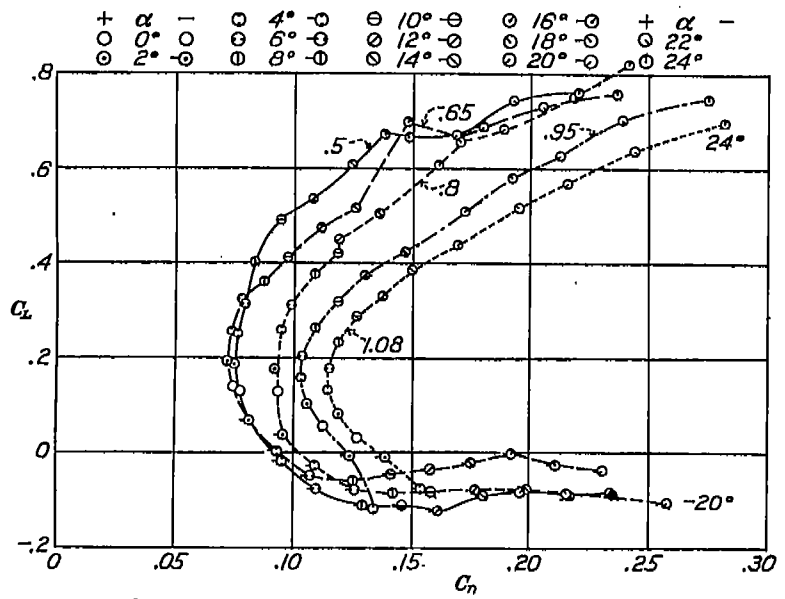


FIGURE 8.—Polar diagrams for airfoil CA16 for five values of  $V/c$

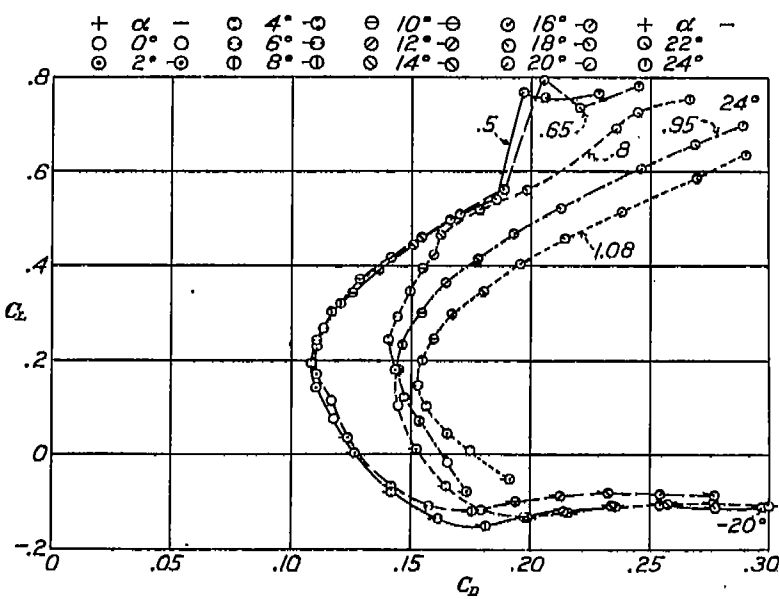


FIGURE 9.—Polar diagrams for airfoil CA20 for five values of  $V/c$

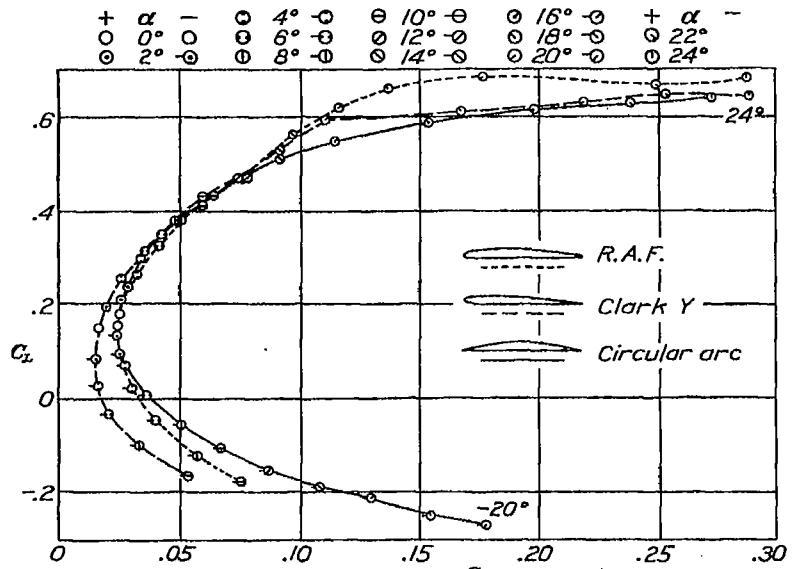


FIGURE 10.—Polar diagrams for airfoils 3R8, C8, and CA8 for  $V/c=0.50$ . Max. ord.=0.08

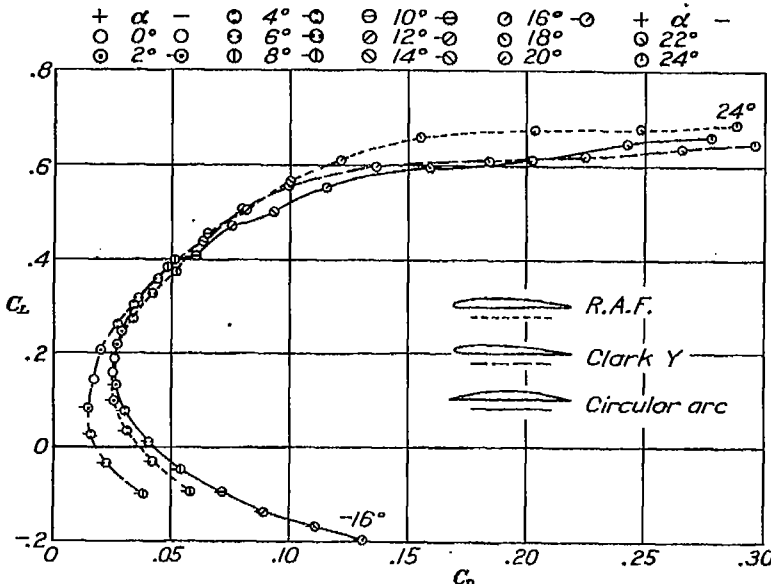


FIGURE 11.—Polar diagrams for airfoils 3R8, C8, and CA8 for  $V/c=0.65$ . Max. ord.=0.08

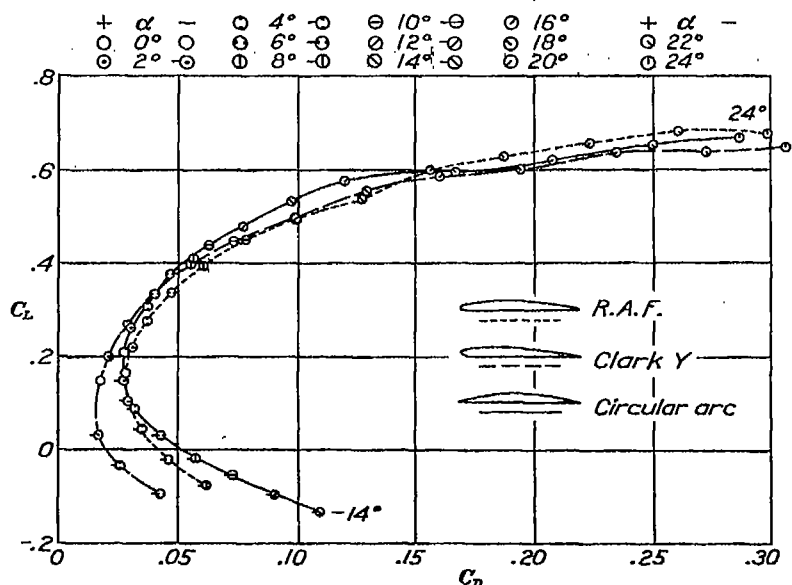


FIGURE 12.—Polar diagrams for airfoils 3R8, C8, and CA8 for  $V/c=0.80$ . Max. ord.=0.08

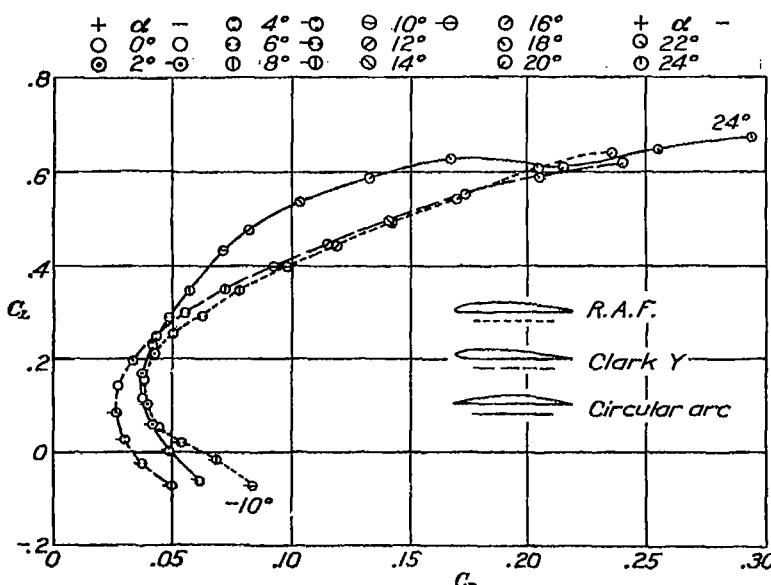


FIGURE 13.—Polar diagrams for airfoils 3R8, C8, and CA8 for  $V/c=0.95$ . Max. ord.=0.08

88800-32

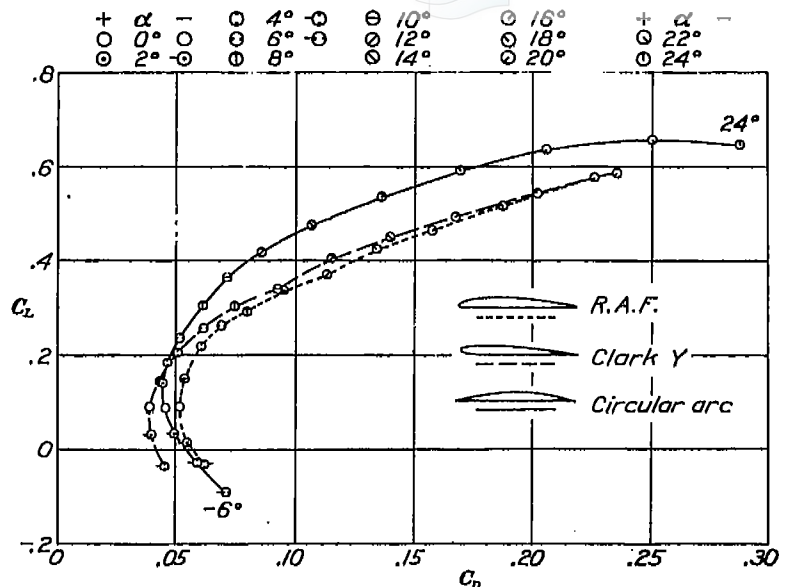


FIGURE 14.—Polar diagrams for airfoils 3R8, C8, and CA8 for  $V/c=1.08$ . Max. ord.=0.08

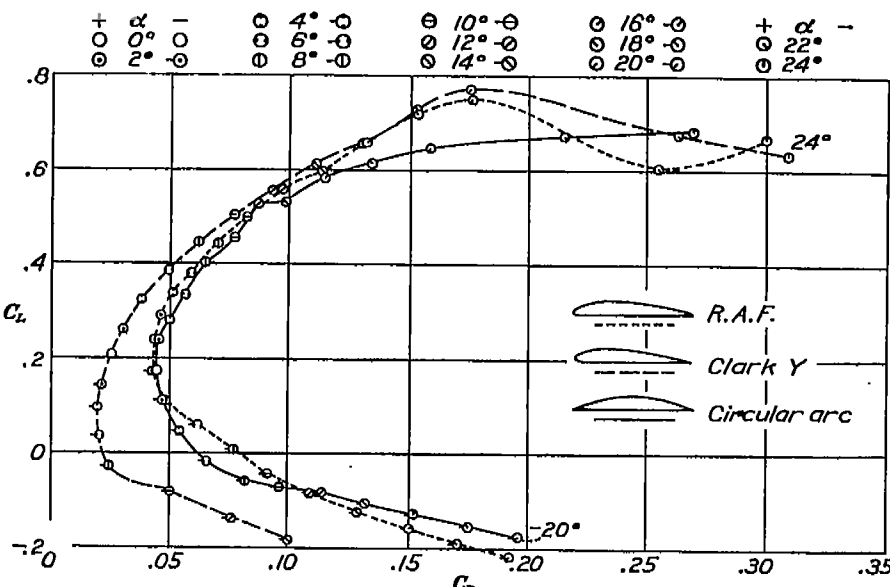


FIGURE 15.—Polar diagrams for airfoils 3R12, C12, and CA12 for  $V/c=0.50$ . Max. ord.=0.12

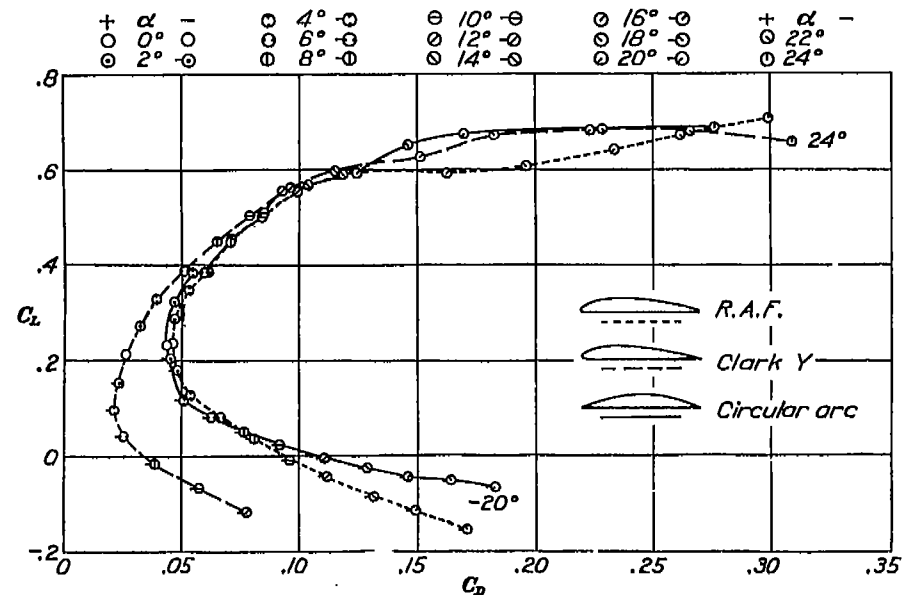


FIGURE 16.—Polar diagrams for airfoils 3R12, C12, and CA12 for  $V/c=0.65$ . Max. ord.=0.12

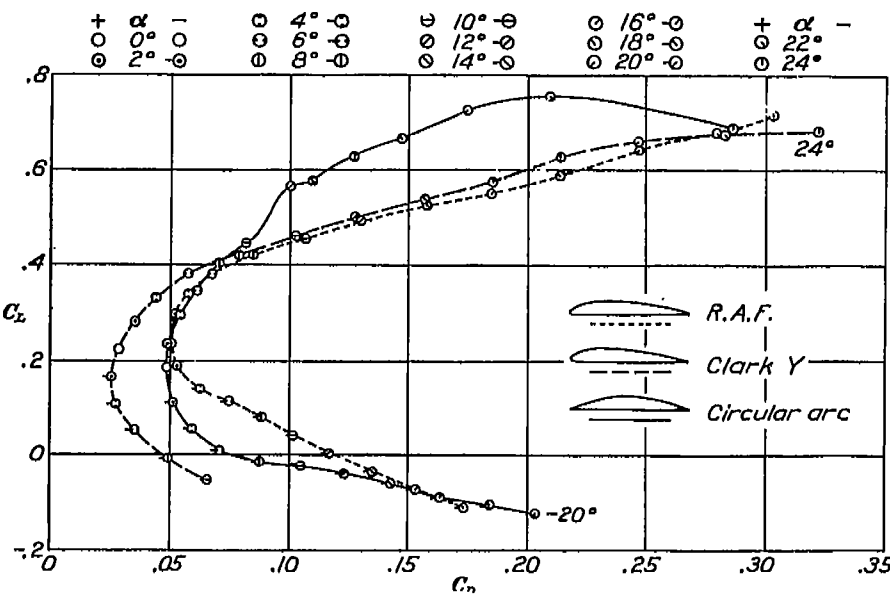


FIGURE 17.—Polar diagrams for airfoils 3R12, C12, and CA12 for  $V/c=0.80$ . Max. ord.=0.12

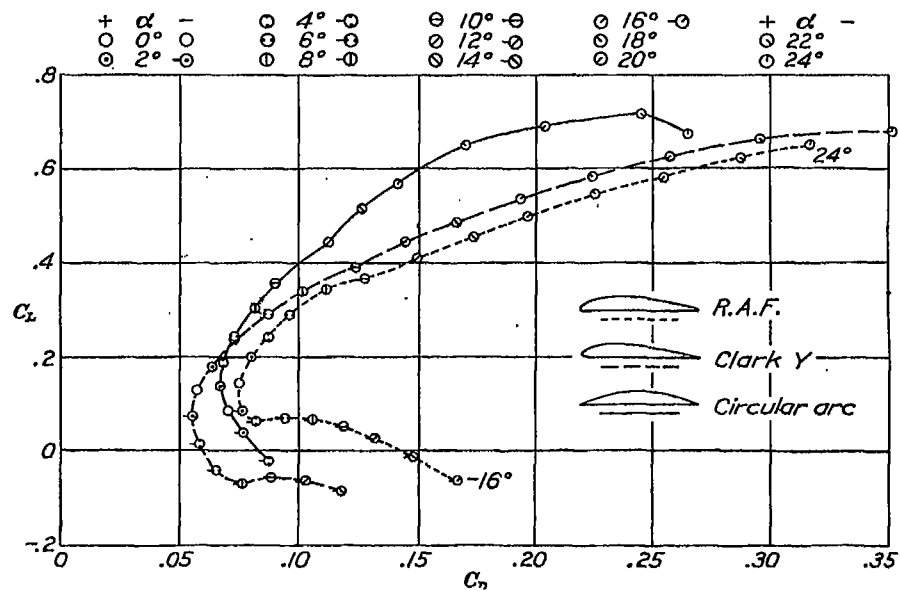


FIGURE 18.—Polar diagrams for airfoils 3R12, C12, and CA12 for  $V/c=0.95$ . Max. ord.=0.12

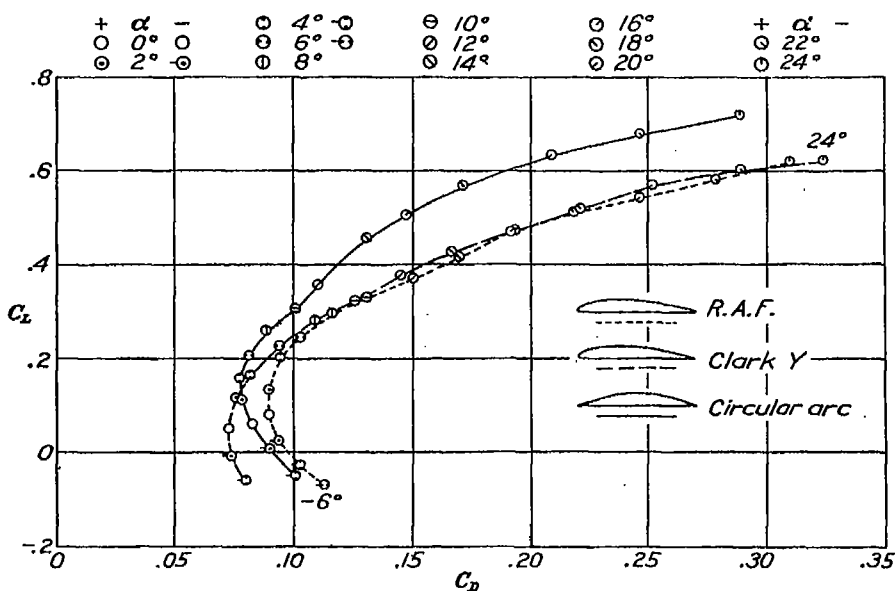


FIGURE 19.—Polar diagrams for airfoils 3R12, C12, and CA12 for  $V/c=1.03$ . Max. ord.=0.12

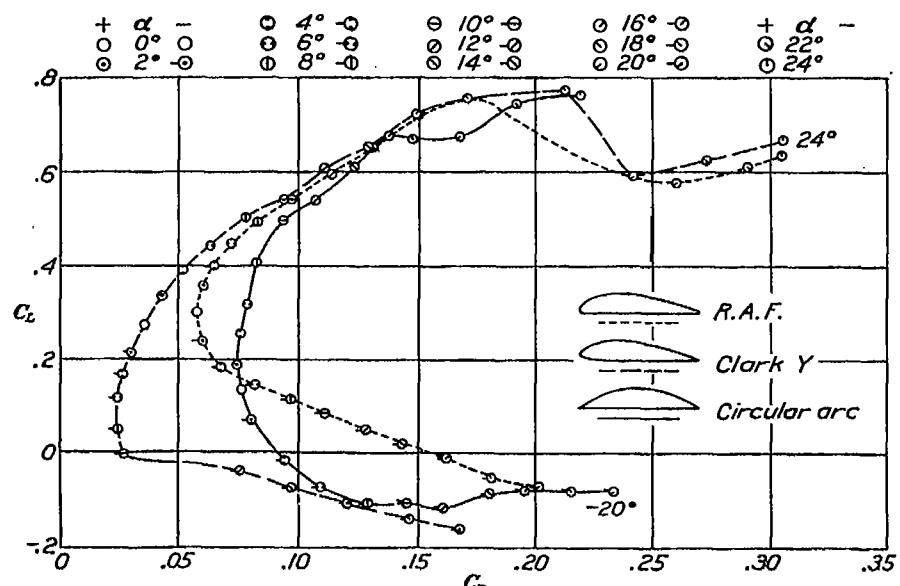


FIGURE 20.—Polar diagram for airfoils 3R16, C16, and CA16 for  $V/c=0.60$ . Max. ord.=0.16

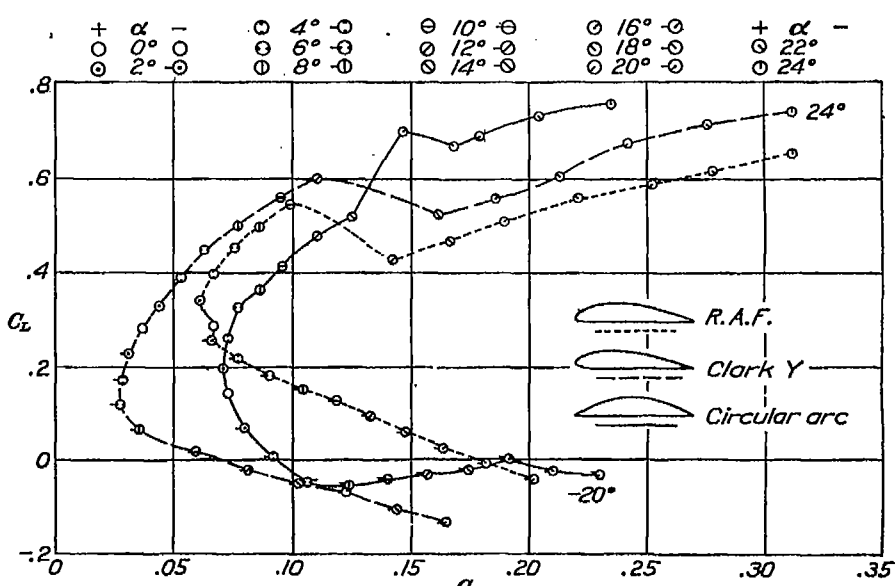


FIGURE 21.—Polar diagrams for airfoils 3R16, C16, and CA16 for  $V/c=0.85$ . Max. ord.=0.16

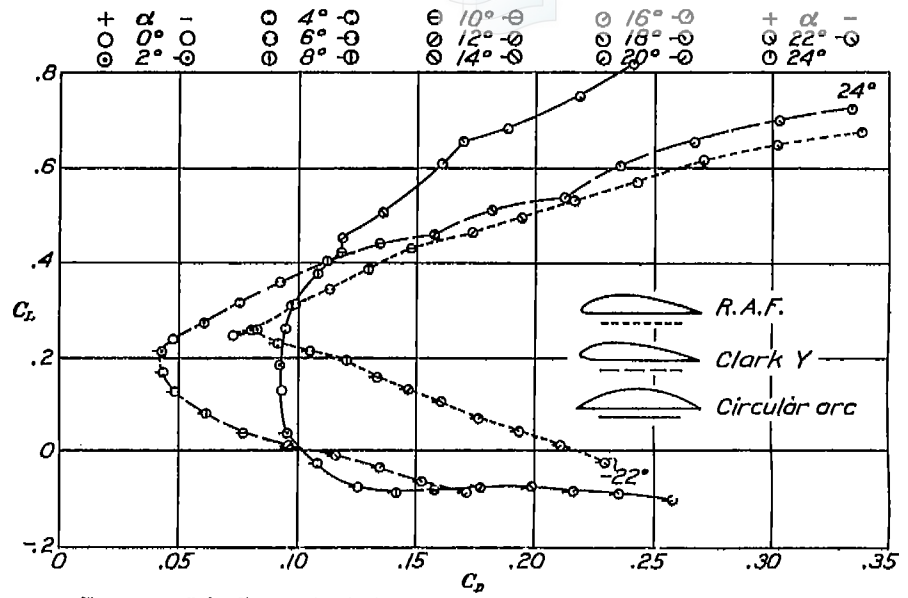


FIGURE 22.—Polar diagrams for airfoils 3R16, C16, and CA16 for  $V/c=0.80$ . Max. ord.=0.16

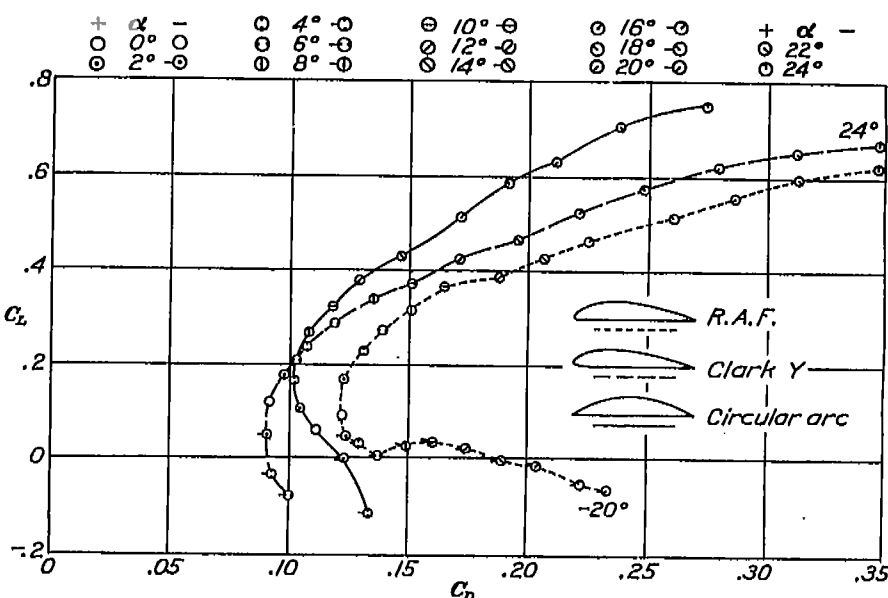


FIGURE 23.—Polar diagrams for airfoils 3R16, C16, and CA16 for  $V/c=0.95$ . Max. ord.=0.16

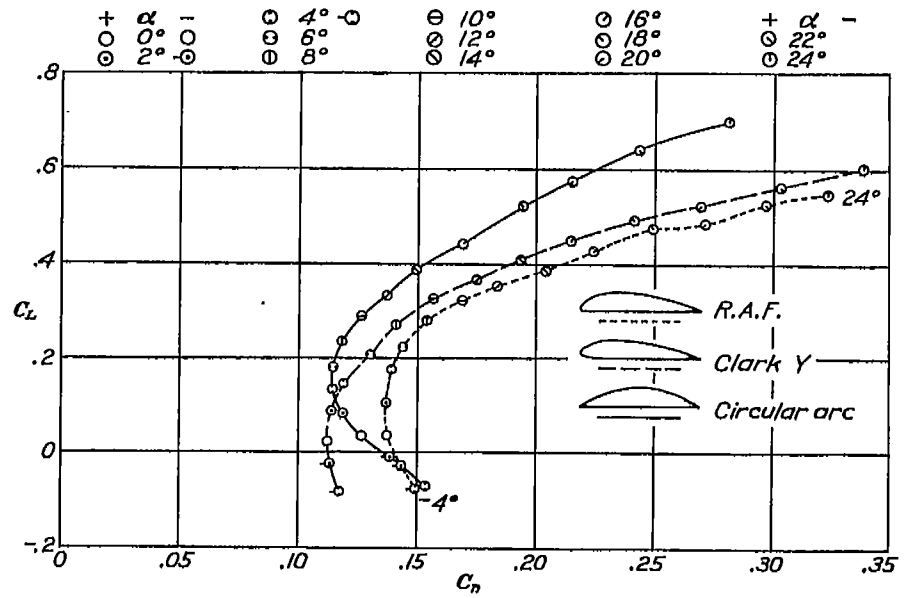


FIGURE 24.—Polar diagrams for airfoils 3R16, C16, and CA16 for  $V/c=1.08$ . Max. ord.=0.16

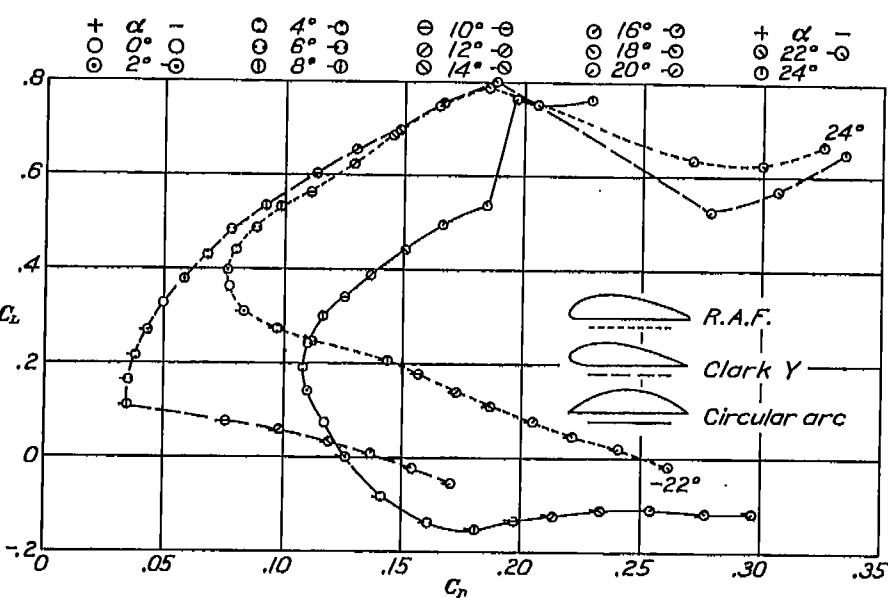


FIGURE 25.—Polar diagrams for airfoils 3R20, C20, and CA20 for  $V/c=0.50$ . Max. ord.=0.16

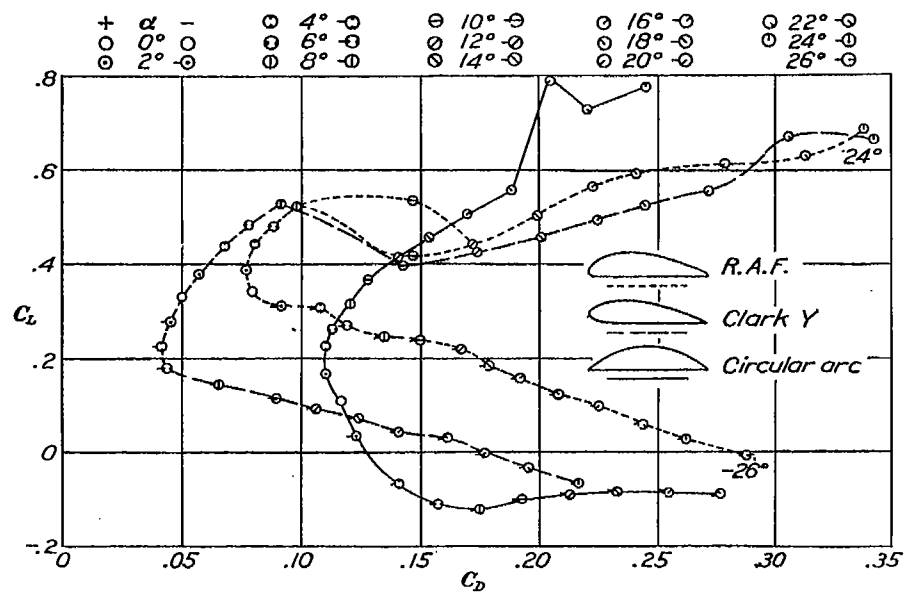


FIGURE 26.—Polar diagrams for airfoils 3R20, C20, and CA20 for  $V/c = 0.65$ . Max. ord. = -0.20

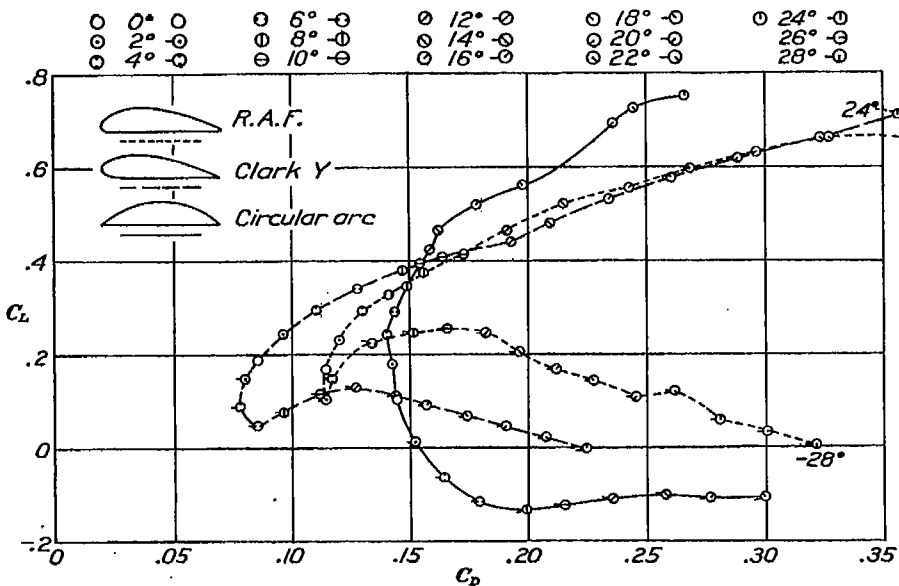


FIGURE 27.—Polar diagrams for airfoils 3R20, C20, and CA20 for  $V/c = 0.80$ . Max. ord. = -0.20

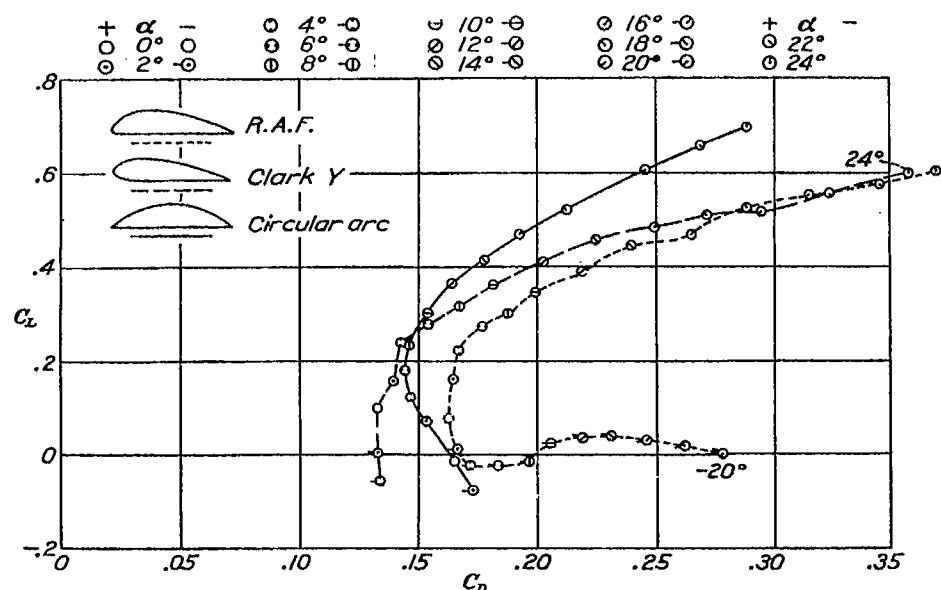


FIGURE 28.—Polar diagrams for airfoils 3R20, C20, and CA20 for  $V/c = 0.95$ . Max. ord. = -0.20

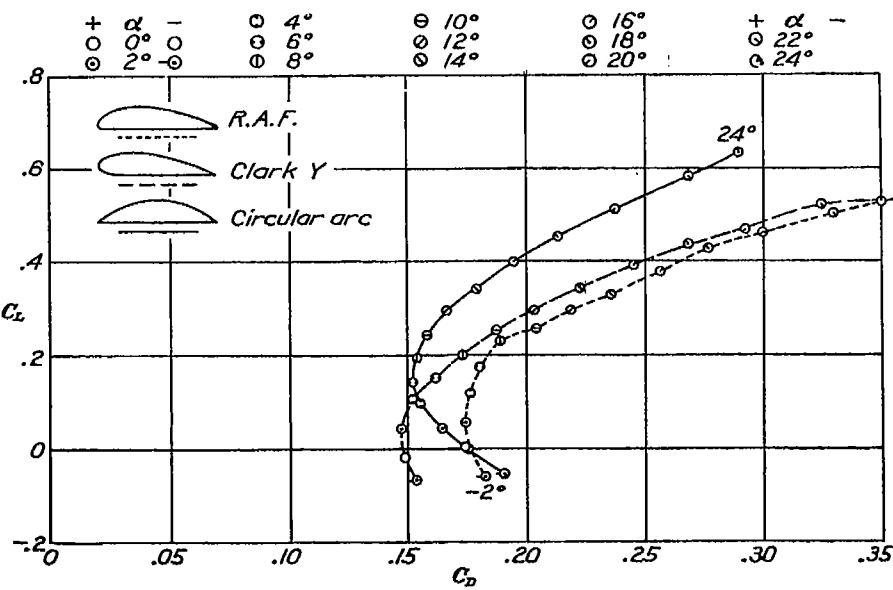


FIGURE 29.—Polar diagrams for airfoils 3R20, C20, and CA20 for  $V/c = 1.06$ . Max. ord. = -0.20

AERODYNAMIC CHARACTERISTICS OF CIRCULAR-ARC AIRFOILS AT HIGH SPEEDS

77

**TABLE I**  
**AIRFOIL CA8**

Lift coefficients, $C_L$										
$V/c$	-20°	-18°	-16°	-14°	-12°	-10°	-8°	-6°	-4°	-2°
0.50	-0.270	-0.251	-0.223	-0.190	-0.154	-0.108	-0.056	0.009	0.071	0.182
.65			-1.197	-1.165	-1.135	-0.911	-0.433	.014	.081	.136
.80					-1.135	-0.986	-0.555	-0.019	.030	.088
.95							-0.080	-0.002	.060	.146
1.08								-0.034	-0.028	.033

Drag coefficients, $C_D$										
$V/c$	0°	2°	4°	6°	8°	10°	12°	14°	16°	20°
0.50	0.179	0.166	0.131	0.100	0.087	0.067	0.052	0.037	0.029	0.025
.65			-1.181	-1.111	-0.900	-0.721	-0.565	-0.411	-0.311	-0.27
.80				-1.110	-0.900	-0.731	-0.558	-0.411	-0.333	-0.28
.95							-0.721	-0.660	-0.51	
1.08										

Lift coefficients,  $C_L$  (above table continued)

$V/c$	0°	2°	4°	6°	8°	10°	12°	14°	16°	20°
0.50	0.181	0.238	0.300	0.352	0.330	0.413	0.471	0.512	0.549	0.618
.65	.194	.250	.306	.359	.402	.409	.472	.501	.554	.612
.80	.206	.259	.307	.374	.400	.433	.476	.520	.573	.617
.95	.117	.169	.228	.289	.347	.431	.477	.534	.588	.608
1.08	.086	.140	.184	.235	.303	.387	.418	.478	.532	.635

Drag coefficients, $C_D$										
$V/c$	0°	2°	4°	6°	8°	10°	12°	14°	16°	20°
0.50	0.026	0.029	0.035	0.043	0.049	0.060	0.075	0.092	0.115	0.199
.65	.027	.030	.035	.045	.052	.061	.076	.094	.116	.203
.80	.028	.031	.038	.047	.057	.068	.078	.098	.120	.209
.95	.038	.058	.042	.049	.058	.071	.083	.104	.133	.215
1.08	.046	.046	.048	.053	.063	.073	.088	.108	.128	.207

AIRFOIL CA8a

Lift coefficients, $C_L$										
$V/c$	-20°	-18°	-16°	-14°	-12°	-10°	-8°	-6°	-4°	-2°
0.50	-0.337	-0.313	-0.292	-0.260	-0.217	-0.173	-0.111	-0.038	0.030	0.094
.65			-1.207	-1.169	-1.128	-0.650	-0.006	.072	.127	
.80				-1.127	-0.868	-0.411	.017	.080	.142	
.95						-1.20	-0.555	.009	.072	
1.08							-0.091	-0.024	.040	

Drag coefficients, $C_D$										
$V/c$	0°	2°	4°	6°	8°	10°	12°	14°	16°	20°
0.50	0.189	0.166	0.142	0.119	0.096	0.074	0.055	0.040	0.030	0.026
.65			-1.112	-1.090	-0.72	-0.584	-0.39	-0.29	-0.26	
.80				-0.91	-0.73	-0.58	-0.44	-0.38	-0.29	
.95					-0.74	-0.58	-0.47	-0.39	-0.30	
1.08						-0.71	-0.59	-0.50	-0.40	

Lift coefficients,  $C_L$  (above table continued)

$V/c$	0°	2°	4°	6°	8°	10°	12°	14°	16°	20°
0.50	0.161	0.213	0.281	0.335	0.369	0.416	0.469	0.524	0.562	0.637
.65	.183	.238	.302	.337	.368	.431	.480	.531	.571	.629
.80	.196	.248	.312	.338	.382	.438	.491	.544	.582	.628
.95	.187	.263	.349	.369	.447	.492	.528	.590	.622	
1.08	.098	.140	.208	.275	.320	.362	.422	.484	.535	.603

Drag coefficients, $C_D$										
$V/c$	0°	2°	4°	6°	8°	10°	12°	14°	16°	20°
0.50	0.026	0.029	0.035	0.040	0.049	0.062	0.078	0.095	0.116	0.202
.65	.028	.029	.036	.042	.050	.063	.079	.098	.124	.208
.80	.029	.032	.038	.044	.053	.066	.082	.102	.127	.216
.95	.034	.038	.043	.051	.059	.070	.087	.112	.148	.223
1.08	.046	.045	.049	.054	.062	.075	.092	.116	.146	.217

TABLE I—Continued

AIRFOIL CA8b

Lift coefficients, $C_L$										
$V/c$	-20°	-18°	-16°	-14°	-12°	-10°	-8°	-6°	-4°	-2°
0.50			-0.318	-0.294	-0.258	-0.215	-0.147	-0.077	-0.016	0.055
.65				-0.222	-0.189	-0.100	-0.039	-0.016	0.038	
.80					-0.132	-0.081	-0.023	-0.043	0.107	
.95						-0.112	-0.047	-0.020	0.124	
1.08							-0.039	-0.018	0.067	

Drag coefficients, $C_D$										
$V/c$	0°	2°	4°	6°	8°	10°	12°	14°	16°	20°
0.50	0.141	0.119	0.098	0.074	0.055	0.040	0.030	0.020	0.010	0.025
.65			-0.094	-0.073	-0.058	-0.042	-0.023	-0.011	0.011	0.025
.80				-0.075	-0.070	-0.064	-0.053	-0.042	-0.032	0.027
.95					-0.070	-0.054	-0.043	-0.032	-0.027	0.037
1.08						-0.068	-0.057	-0.048	-0.040	0.049

Lift coefficients,  $C_L$  (above table continued)

$V/c$	0°	2°	4°	6°	8°	10°	12°	14°	16°	20°
0.50	0.128	0.104	0.086	0.063	0.043	0.030	0.020	0.013	0.009	0.011
.65	.152	.190	.252	.299	.355	.417	.462	.512	.554	.611
.80	.159	.203	.250	.314	.370	.431	.473	.522	.549	.613
.95	.160	.192	.254	.316	.391	.433	.472	.536	.593	.659
1.08	.115	.164	.227	.270	.324	.367	.428	.484	.543	.662

Drag coefficients,  $C_D$										
$V/c$	0°	2°	4°	6°	8°	10°	12°	14°	16°	20°




<tbl\_r cells="11" ix="4" max

TABLE I—Continued  
 AIRFOIL CA12a

Lift coefficients, $C_L$											
$V/c$	$-20^\circ$	$-18^\circ$	$-16^\circ$	$-14^\circ$	$-12^\circ$	$-10^\circ$	$-8^\circ$	$-6^\circ$	$-4^\circ$	$-2^\circ$	
0.50	-0.217	-0.204	-0.155	-0.144	-0.109	-0.090	-0.069	-0.000	0.069	0.187	
.65	-0.164	-0.123	-0.097	-0.060	-0.045	-0.017	.027	.085	.117	.186	
.80											
.95											
1.08											
Drag coefficients, $C_D$											
0.50	0.200	0.179	0.151	0.183	0.113	0.093	0.076	0.060	0.047	0.040	
.65	.192	.169	.147	.128	.108	.089	.073	.057	.046	.042	
.80											
.95											
1.08											
Lift coefficients, $C_L$ (above table continued)											
$V/c$	$0^\circ$	$2^\circ$	$4^\circ$	$6^\circ$	$8^\circ$	$10^\circ$	$12^\circ$	$14^\circ$	$16^\circ$	$20^\circ$	
0.50	0.186	0.251	0.320	0.391	0.450	0.528	0.530	0.558	0.586	0.674	
.65	.244	.307	.358	.403	.449	.523	.523	.566	.612	.678	
.80	.208	.270	.328	.363	.425	.478	.542	.578	.616	.716	
.95	.094	.141	.191	.261	.304	.387	.480	.518	.581	.703	
1.08	.070	.121	.168	.218	.280	.309	.400	.465	.512	.617	
Drag coefficients, $C_D$											
0.50	0.041	0.043	0.049	0.057	0.069	0.082	0.084	0.098	0.116	0.181	
.65	.041	.046	.051	.060	.070	.086	.089	.106	.124	.171	
.80	.046	.048	.053	.062	.072	.083	.089	.109	.127	.178	
.95	.067	.068	.066	.073	.081	.094	.110	.122	.146	.216	
1.08	.078	.074	.074	.078	.085	.094	.111	.127	.149	.215	

AIRFOIL CA12b

Lift coefficients, $C_L$											
$V/c$	$-20^\circ$	$-18^\circ$	$-16^\circ$	$-14^\circ$	$-12^\circ$	$-10^\circ$	$-8^\circ$	$-6^\circ$	$-4^\circ$	$-2^\circ$	
0.50	-0.208	-0.189	-0.163	-0.131	-0.105	-0.079	-0.043	0.004	0.078	0.155	
.65	-0.177	-0.146	-0.123	-0.093	-0.062	-0.039	.042	.092	.146	.205	
.80											
.95											
1.08											
Drag coefficients, $C_D$											
0.50	0.192	0.170	0.147	0.128	0.108	0.088	0.072	0.056	0.046	0.040	
.65	.189	.167	.148	.124	.107	.089	.071	.058	.046	.041	
.80	.176	.156	.136	.116	.096	.079					
.95											
1.08											
Lift coefficients, $C_L$ (above table continued)											
$V/c$	$0^\circ$	$2^\circ$	$4^\circ$	$6^\circ$	$8^\circ$	$10^\circ$	$12^\circ$	$14^\circ$	$16^\circ$	$20^\circ$	
0.50	0.217	0.268	0.333	0.384	0.453	0.487	0.511	0.558	0.603	0.680	
.65	.240	.312	.385	.414	.452	.472	.513	.560	.613	.650	
.80	.226	.272	.338	.378	.462	.480	.508	.568	.628	.684	
.95	.097	.147	.210	.260	.381	.421	.487	.521	.579	.614	
1.08	.063	.123	.179	.231	.313	.346	.395	.450	.513	.538	
Drag coefficients, $C_D$											
0.50	0.039	0.042	0.048	0.056	0.066	0.072	0.084	0.090	0.119	0.167	
.65	.041	.045	.052	.061	.068	.075	.088	.106	.128	.187	
.80	.048	.047	.053	.061	.073	.080	.091	.108	.130	.214	
.95	.068	.063	.064	.070	.082	.091	.107	.124	.153	.221	
1.08	.077	.074	.074	.079	.087	.095	.112	.131	.163	.220	

Drag coefficients,  $C_D$

Lift coefficients, $C_L$											
$V/c$	$-20^\circ$	$-18^\circ$	$-16^\circ$	$-14^\circ$	$-12^\circ$	$-10^\circ$	$-8^\circ$	$-6^\circ$	$-4^\circ$	$-2^\circ$	
0.50	-0.084	-0.084	-0.082	-0.089	-0.121	-0.110	-0.110	-0.078	-0.019	0.067	
.65	-.032	-.025	-.001	-.023	-.033	-.045	-.057	-.048	-.003	.087	
.80	-.102	-.089	-.085	-.076	-.076	-.081	-.085	-.077	-.028	.038	
.95											
1.08											
Drag coefficients, $C_D$											
0.50	0.284	0.216	0.197	0.181	0.161	0.146	0.129	0.110	0.098	0.082	
.65	.231	.211	.192	.175	.158	.141	.125	.107	.093	.081	
.80	.258	.236	.217	.198	.177	.160	.142	.126	.109	.096	
.95											
1.08											
Lift coefficient, $C_L$ (above table continued)											
$V/c$	$0^\circ$	$2^\circ$	$4^\circ$	$6^\circ$	$8^\circ$	$10^\circ$	$12^\circ$	$14^\circ$	$16^\circ$	$20^\circ$	
0.50	0.131	0.186	0.251	0.313	0.402	0.403	0.536	0.606	0.674	0.873	
.65	.140	.193	.255	.322	.356	.409	.474	.514	.597	.887	
.80	.130	.180	.239	.312	.378	.421	.451	.507	.608	.885	
.95	.059	.104	.162	.204	.264	.320	.377	.427	.510	.889	
1.08	.033	.082	.132	.178	.232	.286	.330	.388	.439	.870	
Drag coefficients, $C_D$											
0.50	0.077	0.075	0.077	0.080	0.083	0.095	0.108	0.125	0.138	0.169	
.65	.074	.072	.074	.078	.087	.097	.111	.128	.148	.180	
.80	.094	.092	.095	.099	.109	.119	.138	.161	.189	.218	
.95	.118	.106	.103	.104	.109	.119	.130	.148	.173	.213	
1.08	.127	.119	.115	.116	.119	.127	.138	.150	.168	.216	
Lift coefficients, $C_L$ (above table continued)											
$V/c$	$0^\circ$	$2^\circ$	$4^\circ$	$6^\circ$	$8^\circ$	$10^\circ$	$12^\circ$	$14^\circ$	$16^\circ$	$20^\circ$	
0.50	0.076	0.141	0.192	0.241	0.301	0.341	0.390	0.443	0.497	0.765	
.65	.111	.168	.226	.264	.317	.366	.413	.468	.505	.792	
.80	.104	.179	.242	.290	.344	.394	.422	.462	.518	.790	
.95	-.018	.070	.121	.177	.232	.299	.362	.412	.467	.795	
1.08	-.008	.043	.100	.145	.199	.245	.298	.345	.402	.714	
Drag coefficients, $C_D$											
0.50	0.118	0.110	0.109	0.111	0.117	0.126	0.127	0.131	0.167	0.198	
.65	.117	.111	.111	.114	.121	.129	.142	.158	.171	.206	
.80	.145	.144	.140	.143	.149	.155	.160	.162	.179	.227	
.95	.166	.154	.147	.145	.148	.154	.164	.179	.193	.246	
1.08	.175	.163	.156	.153	.155	.159	.167	.181	.199	.238	

TABLE I—Continued  
 AIRFOIL CA16